



Cite this: *J. Anal. At. Spectrom.*, 2023, **38**, 1238

# Online monitoring of atmospheric krypton-85 with hourly time resolution†

Yan-Qing Chu,  Wen-Hao Wang, Xi-Ze Dong, Chao Gao, Ji-Qiang Gu, Shui-Ming Hu,  Wei Jiang,\* Si-Yu Liu, Zheng-Tian Lu, Florian Ritterbusch, Guo-Min Yang\* and Lei Zhao

$^{85}\text{Kr}$  is a major radioactive byproduct released during nuclear fuel reprocessing and an important atmospheric indicator for nuclear safety and environmental monitoring. In this work, we report on online monitoring of atmospheric  $^{85}\text{Kr}$  activities with time resolution of 1.5 hours. An automated Kr purification system and an atom trap based  $^{85}\text{Kr}$  measurement system work synchronously in the experiment. The Kr purification system features temperature-controlled cryogenic distillation and gas chromatography, which allows direct sampling of ambient air and continuous operation. The separated Kr is fed into an atom trap capable of measuring the abundance of  $^{85}\text{Kr}$  with micro-L size Kr samples. The sample consumption is 3 L STP of air per measurement with a 1.5 hour processing time. Compared to the conventional monitoring method based on proportional counting, both the measurement time and sample size (10 m<sup>3</sup> and 1 week) are reduced by several orders of magnitude. The  $^{85}\text{Kr}$  analysis technology demonstrated in this work allows analysis of atmospheric  $^{85}\text{Kr}$  activities with hourly resolution, enabling applications such as online monitoring of nuclear fuel reprocessing plants and tracing of atmospheric circulation patterns.

Received 29th September 2022  
 Accepted 21st April 2023

DOI: 10.1039/d2ja00318j

rs.c.li/jaas

## 1 Introduction

$^{85}\text{Kr}$  is an important gas radioactive byproduct of the nuclear industry. It has a half-life of 10.74 years and beta decays to  $^{85}\text{Rb}$ .<sup>1</sup> Today the largest  $^{85}\text{Kr}$  emission sources are the nuclear fuel reprocessing plants in the UK and France.<sup>2</sup> Compared to pre-1950s, its concentration in the air has increased by more than 5–6 orders of magnitude. Its current activity in the air is about 1.5 Bq m<sup>-3</sup>.<sup>3,4</sup> The atmospheric  $^{85}\text{Kr}$  has been monitored because of its potential impacts on human health and the environment.<sup>5–7</sup> Being a good environmental tracer,  $^{85}\text{Kr}$  is also used to date young groundwater and seawater.<sup>8–15</sup> Moreover,  $^{85}\text{Kr}$  has been suggested for validating atmospheric transport models and for investigating atmospheric and inter-hemispheric transport processes.<sup>7,16–19</sup>

The conventional method for measuring atmospheric  $^{85}\text{Kr}$  activity is proportional counting. Due to the extremely low concentrations of  $^{85}\text{Kr}$  in the atmosphere (isotopic abundance  $\sim 2 \times 10^{-11}$ ), large amounts of air (10 m<sup>3</sup> in one week) are needed.<sup>20,21</sup> It is possible to measure smaller air samples (a few liters) in underground low level counting (LLC) laboratories. However, the long measurement time (a few days) limits the

throughput and online operations.<sup>22,23</sup> Therefore the LLC method is often used for measuring groundwater samples rather than measuring air samples. The laser-based Atom Trap Trace Analysis (ATTA) technology is a method for measuring the  $^{85}\text{Kr}$  activities of small air samples (liters) quickly.<sup>24–28</sup> In ATTA, the  $^{85}\text{Kr}$  atoms are selectively captured by a resonant laser trap and counted by detecting their fluorescence. Analysis of  $^{85}\text{Kr}$  in environmental samples with ATTA has been realized.<sup>26,27</sup> More recently, fast ATTA analysis of  $^{85}\text{Kr}$  activities at the 3% precision level on a 1 L STP (Standard Temperature and Pressure) air sample with 1.5 hour turnaround time has been realized in Gao *et al.* 2021.<sup>29</sup> However, continuous operation has not been possible in that work since air sampling, Kr extraction and  $^{85}\text{Kr}$  measurement work separately on discrete sample with attended operation. It is worth further developing to realize online measurement of atmospheric  $^{85}\text{Kr}$  activities. Such capability can be used to monitor nuclear fuel reprocessing plants remotely, validate air diffusion models and evaluate impact zones in case of a nuclear accident.<sup>7</sup> Moreover, weekly averaged atmospheric  $^{85}\text{Kr}$  activities in central Europe reported in previous studies showed large fluctuations above the baseline.<sup>2,3,19</sup> Therefore for monitoring stations near the source, higher temporal resolution can allow more effective detections and reveal more details of the emission pattern.

We report on online monitoring of atmospheric  $^{85}\text{Kr}$  activities based on the ATTA technology.<sup>29</sup> An automated system capable of direct sampling of the ambient air and measuring

CAS Center for Excellence in Quantum Information and Quantum Physics, School of Physical Sciences, University of Science and Technology of China, China. E-mail: [wjiang1@ustc.edu.cn](mailto:wjiang1@ustc.edu.cn); [yanggm@ustc.edu.cn](mailto:yanggm@ustc.edu.cn)

† Electronic supplementary information (ESI) available. See DOI: <https://doi.org/10.1039/d2ja00318j>

the isotopic abundance of  $^{85}\text{Kr}$  has been realized. The system links the purification setup and the ATTA instrument directly and allows them to work in a synchronized manner. To increase time resolution, we developed a purification setup that features a combination of cryogenic distillation and gas chromatography (GC) and a correction model to correct the memory effect in the ATTA system. We demonstrate unattended continuous measurement of atmospheric  $^{85}\text{Kr}$  activities for over 24 hours. The measurement precision is about 3% with a time resolution of 1.5 hours and the air sample consumption for a single measurement is 3 L STP.

## 2 Experimental

The measurement system consists of two major parts. The first part is an automated air sampling and Kr separation system that can directly sample the air and perform Kr extraction. The second part is an automated ATTA instrument that can perform  $^{85}\text{Kr}$  atom counting on Kr samples. These two parts are linked to each other and operate synchronously under computer control.

### 2.1 The automatic air sampling and Kr separation system

The automatic Kr separation system consists of three stages: a temperature-controlled cryogenic distillation stage, a gas chromatography stage, and a getter & collection stage. Fig. 1 is the schematic diagram. The whole setup is made of stainless

steel parts based on press fitting tubing systems. All valves are air-actuated and controlled by a computer.

Before entering the main separation sections, the air sample flows through a U-shaped trap filled with molecular sieve (MS5A) to remove  $\text{H}_2\text{O}$  and  $\text{CO}_2$ . About 3 L STP of dry air are frozen into the temperature controlled trap (trap 1) from the right side through a Mass Flow Controller (MFC1). During the cryogenic distillation, trap 1 is pumped from the left side. The same MFC1 is used to control the flow speed at  $500 \text{ mL min}^{-1}$  for both, freezing and pumping.

Trap 1 is made of a U-shaped stainless steel tube (4 mm inner diameter, 30 cm length) filled with activated charcoal (grain size, no. 16–32; 3 g). A layer of heating wire is wrapped around the cold trap for temperature control purposes. During operation, the cold trap is immersed in an alcohol tank cooled by liquid nitrogen. The temperature of the trap is monitored by a platinum resistance temperature sensor and regulated by a temperature controller (LakeShore Model 331). By changing the power applied to the heating wire, the temperature of the trap can be varied between 83 K and 370 K with a stability of 1 K.

**2.1.1 Temperature-controlled cryogenic distillation.** In order to remove the bulk gas other than Kr in trap 1, temperature-controlled distillation is performed. During this process, the temperature of the cold trap is kept at a fixed temperature (100–120 K) while being pumped by a dry pump. Because  $\text{N}_2$ ,  $\text{O}_2$  and Ar have lower boiling points than Kr, their vapor pressure will be higher than that of Kr during the

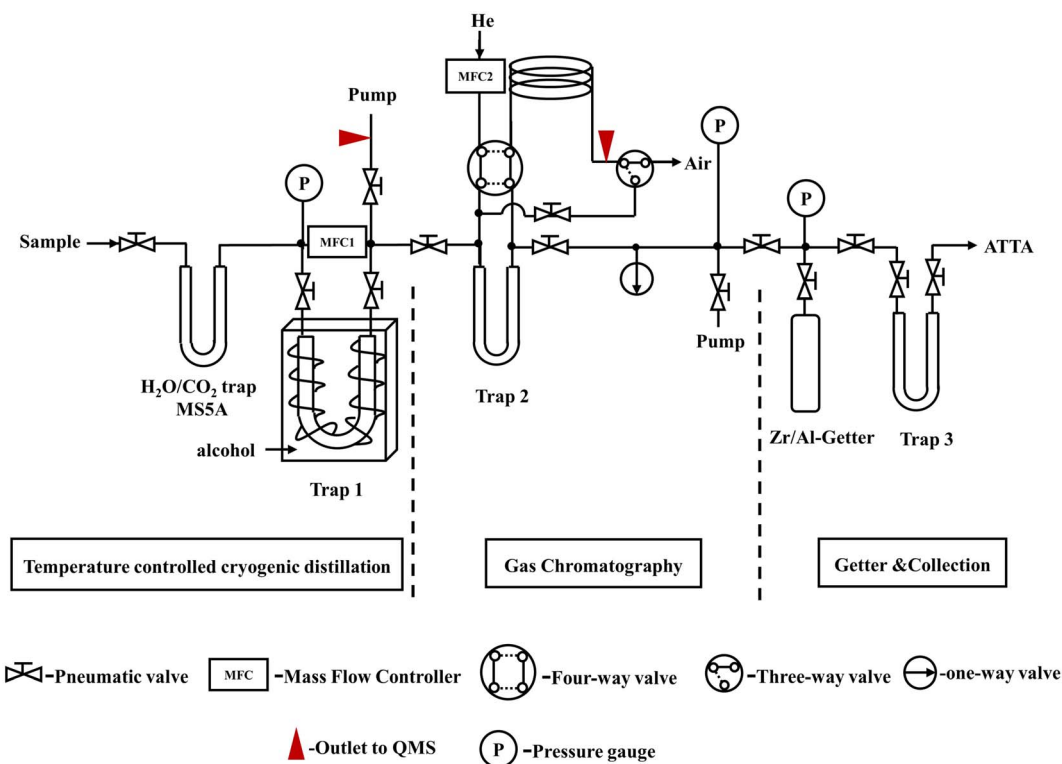


Fig. 1 Schematic of the automatic Kr separation system. About 3 L STP of dry air are frozen into the temperature controlled trap (trap 1) for the cryogenic distillation. Then residual gas is separated by two successive gas chromatography (GC) cycles. Krypton gas is collected in trap 3 waiting for ATTA measurement.

distillation. As a result more  $N_2$ ,  $O_2$  and Ar will be removed than Kr. The remaining gas in the trap is therefore enriched in Kr.<sup>5,30–32</sup>

The distillation method has several advantages over the recently reported Kr separation method based on Ti-oven and GC in terms of online monitoring of atmospheric  $^{85}Kr$ .<sup>29</sup> First, it only consumes liquid nitrogen, whereas the Ti-oven needs to be refilled with Ti sponges after processing a certain amount of air (the air processing capacity of Ti sponges is about 60 L STP per kg). Second, the cryogenic distillation can remove not only most of  $N_2$  and  $O_2$ , but also part of Ar. As a result this reduces the number of GC cycles required to separate Kr from Ar.

After the distillation the gas composition is analyzed by a quadrupole mass spectrometer (QMS). Fig. 2 shows the Kr enrichment factor and the Kr recovery under different distillation temperatures. Here, the Kr enrichment factor is defined as the ratio of the Kr volume fraction before and after the distillation. From Fig. 2 it can be seen that the Kr enrichment factor is quite sensitive to the distillation temperature between 103 K to 108 K. A higher distillation temperature results in a higher Kr enrichment factor. Above 108 K (up to 113 K) the Kr enrichment factor levels off. On the other hand the Kr recovery decreases at higher distillation temperature, as more Kr is pumped away during the distillation. We choose 109 K as the final working temperature since it is a good balance between the Kr enrichment and the recovery. Under this condition, the initial 3 L STP air sample is reduced to about 10 mL STP. The Kr enrichment factor can be estimated as follows. The Kr recovery is about  $48 \pm 6\%$  (see Table 1), which is mainly determined by the efficiency of the cryogenic distillation step, as the Kr losses are negligible during the GC steps. From these numbers, the Kr enrichment factor in the cryogenic distillation step is  $3 \text{ L}/0.01 \text{ L} \times 0.48 \approx 140$ .

The isotopic fractionation during the distillation is estimated to be less than 1%,<sup>30,33</sup> which is much smaller than the uncertainty of the  $^{85}Kr$  activity measurement later on, and therefore can be neglected.

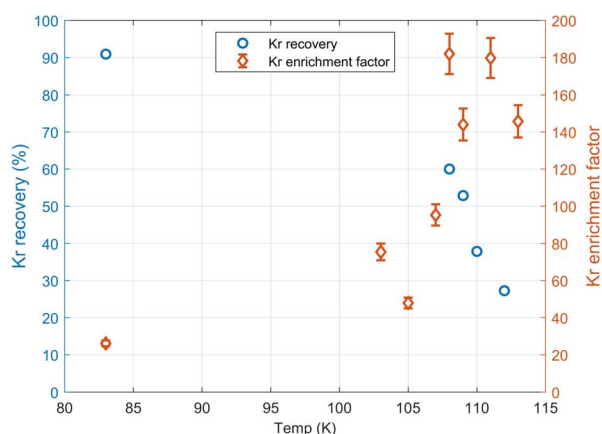


Fig. 2 Kr enrichment factor and Kr recovery at different cryogenic distillation temperatures. The typical error for the Kr recovery measurement is 6%. Limited by the construction of the setup, the enrichment factors and the recovery were measured in the purification system and the ATTA system respectively in separate experiments.

Table 1 Typical performance of the automated Kr separation system

Air sample size (L STP)	Kr extracted ( $\mu\text{L}$ STP)	Recovery (%)	Purity (%)	Time (min)
2.8	1.7	55	81	80
2.7	1.3	44	80	73
2.7	1.3	44	80	79
2.8	1.3	42	79	75
2.7	1.6	54	80	78

Upon the end of the temperature-controlled cryogenic distillation, trap 1 is heated to 370 K. The released gas is then transferred completely into trap 2, a cold trap (same dimensions as trap 1) immersed in liquid nitrogen, before the following gas chromatography.

**2.1.2 Gas chromatography.** At the GC stage, a modified commercial gas chromatography instrument (FULI GC9790plus) is used for further Kr separation. The separation column is a stainless steel tube (4 mm inner diameter, 3 m length) filled with 30–60-mesh molecular sieves 5A and kept at a constant temperature about 333 K in an insulation box. At the beginning of the GC cycle, helium (99.999% purity) carrier gas flows through the four-way valve and trap 2 at  $85 \text{ mL min}^{-1}$  controlled by MFC2. At the same time, trap 2 is heated and kept at 313 K in order to transfer the enriched gas sample completely into the separation column. After the gas leaves trap 2, the trap is cooled by liquid nitrogen again so that it can recollect the Kr gas coming out of the GC. The entire gas separation procedure is monitored by a QMS. At the end of the GC cycle, the three-way valve is switched to steer the gas to trap 2 right before the Kr gas comes out of the separation column. This allows trap 2 to recapture the Kr from the separation column. Depending on the needs of the separation, multiple GC cycles can be carried out in the experiment.

In order to have a good separation between Kr and other gases, two GC cycles are implemented. Fig. 3 shows the gas composition changes for a typical run. The shaded regions mark the period where the gas samples are re-collected in the liquid nitrogen cooled trap 2. After two GC cycles, the remaining gas contains about 1.4  $\mu\text{L}$  STP of Kr and tens of  $\mu\text{L}$  of active gases ( $N_2$ ,  $O_2$ ). To remove the residual active gases, the sample

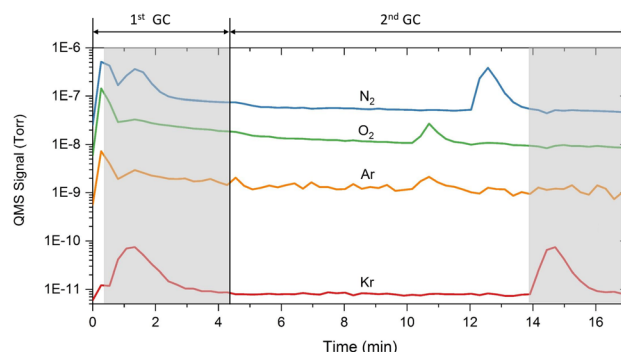


Fig. 3 Two gas chromatography cycles monitored by the QMS. In the shaded area, Kr is collected into trap 2.

then passes through a Zr/Al getter before it is collected into trap 3.

Table 1 shows a few typical runs of the Kr separation system. Krypton can be extracted with efficiency >40% and a purity around 80% from 3 L STP of air. This corresponds to more than 1.2  $\mu\text{L}$  STP krypton and can be readily measured by the ATTA system.

## 2.2 $^{85}\text{Kr}$ activity measurement by the Atom Trap Trace Analysis (ATTA) system

The separated Kr sample in trap 3 is fed into the ATTA instrument for  $^{85}\text{Kr}$  isotopic abundance measurement. ATTA is an ultra-sensitive tracer analysis method based on laser trapping and atom counting. It is capable of detecting  $^{85}\text{Kr}$  at  $10^{-14}$  abundance level.<sup>25,29</sup> During the analysis the atoms of the target  $^{85}\text{Kr}$  isotope are selectively steered by lasers and trapped in a Magneto-Optical-Trap (MOT). The number of the  $^{85}\text{Kr}$  atoms in the MOT is counted by detecting their fluorescence. The details about the apparatus can be found in Gao *et al.* 2021.<sup>29</sup> The ATTA instrument is capable of capturing and measuring different Kr isotopes selectively. During the analysis, the rare  $^{85}\text{Kr}$  isotope is measured by the atom counting method while the reference  $^{83}\text{Kr}$  isotope is measured by the quench fluorescence method.<sup>25</sup> Based on these measurements the  $^{85}\text{Kr}/^{83}\text{Kr}$  ratio of the sample is calculated. The ATTA instrument is calibrated with a series of standard Kr samples with known  $^{85}\text{Kr}$  isotopic abundances. The measured  $^{85}\text{Kr}/^{83}\text{Kr}$  ratio can be converted to the isotopic abundance of  $^{85}\text{Kr}$  in the Kr sample and the  $^{85}\text{Kr}$  activity in the original air sample. The isotopic abundance of the  $^{85}\text{Kr}$  is reported in units of  $\text{dpm cm}^{-3}$  (decay per minutes per cubic centimeter of Kr) following the tradition of the LLC (Low-Level Counting) community. The conversion between the isotopic abundance and  $\text{dpm cm}^{-3}$  is  $100 \text{ dpm cm}^{-3} = 3.03 \times 10^{-11}$ . The  $^{85}\text{Kr}$  activity in the air can be calculated as well using the latest measured Kr concentration in the air ( $1.099 \pm 0.009 \text{ ppm}$ ).<sup>34</sup> The conversion is  $100 \text{ dpm cm}^{-3} = 1.83 \text{ Bq m}^{-3}$  ( $\text{Bq m}^{-3}$ , becquerels per cubic meter of air).

## 2.3 Measurement protocol

Online monitoring of the atmospheric  $^{85}\text{Kr}$  activity was carried out in the laboratory in Hefei, China on Aug. 17–18 2020, lasting 30 hours. The experiment was performed under the following protocol. During the online measurement, samples were collected and measured successively. The operation of the Kr separation system and the ATTA measurement system were synchronized during the experiment. While a sample is being analyzed by the ATTA system, the next air sample is being purified by the Kr separation system. To ensure that the sample measured is from the ambient air, a tube is plugged into the vent of the laboratory room, which brings fresh air from outside. The air was sampled through the tube under the control of a Mass Flow Controller. For each sampling, about 3 L STP of air was collected in 6 min. As the variation of the atmospheric  $^{85}\text{Kr}$  activity in Hefei is small, standard samples with  $^{85}\text{Kr}$  activities significantly different from the air samples were substituted in the measurement queue during online

measurement to test the sensitivity of the system and the effect of cross-sample contamination. The standard samples (labelled Kr2007 and Kr2015 hereafter) were prepared by mixing commercial Kr gas with ultra-high purity nitrogen (99.999% purity), so that the Kr volume fraction is similar to the air. These commercial Kr gases were acquired in 2007 and 2015. Their activities are measured in our laboratory using the ATTA instrument ( $34.51 \pm 0.24 \text{ dpm cm}^{-3}$  and  $54.95 \pm 0.59 \text{ dpm cm}^{-3}$  in August 2020, respectively). The  $^{85}\text{Kr}$  activities of these two Kr samples are much lower than the Kr in the modern air of 2020 in Hefei (around  $80 \text{ dpm cm}^{-3}$ ).

## 3 Results and discussion

The online monitoring results are displayed in Fig. 4. The open symbols are data obtained directly from the measurements. The data show that the  $^{85}\text{Kr}$  activities of the Hefei air (blue open circles) are relatively stable over the time of the online monitoring experiment. The activities of the two standard Kr samples (orange and green open circles), are much lower, as expected. The uncorrected results for the two standard Kr samples are all significantly higher than their expected values (orange and green dashed lines), due to cross-sample contamination. This is not surprising as there is no Xe discharge cleaning process to reduce the cross-sample contamination between successive measurements as in the normal procedures of ATTA.<sup>35</sup> To mitigate this problem, we have developed a model to make corrections to the results and remove the effect due to the cross-sample contaminations.

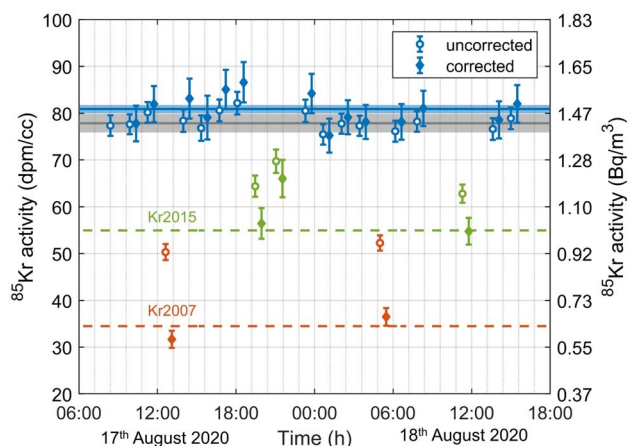


Fig. 4 Results of the online monitoring experiment of atmospheric  $^{85}\text{Kr}$  activities. Open circles are uncorrected results from the measurements. Solid diamonds are results after cross-sample contamination corrections (for clarity, the data points after correction are shifted right horizontally by 0.5 h). Blue: Hefei air samples; orange: standard Kr sample, Kr2007; green: standard Kr sample, Kr2015. Orange and green dashed lines are expected  $^{85}\text{Kr}$  activities of the Kr2007 and Kr2015 standard samples respectively. The blue shaded area is the average of all air samples with contamination corrections. The gray shaded area is the weekly average of the atmospheric  $^{85}\text{Kr}$  activity based on measurement on air collected from Aug. 14, 2020 to Aug. 21, 2020. The atmospheric  $^{85}\text{Kr}$  activities on the right are calculated based on the Kr concentration in the air ( $1.099 \pm 0.009 \text{ ppm}$ ).<sup>34</sup>

### 3.1 The correction model

The cross-sample contamination can be modeled as a binary mixing process between the sample Kr gas and the Kr contaminant outgassed into the vacuum system during the measurement. The true ratio of  $^{85}\text{Kr}/^{83}\text{Kr}$  of the sample Kr gas ( $R_{\text{sample}}$ ) can be expressed as,

$$R_{\text{sample}} = \frac{R_{\text{raw}} - \eta R_{\text{con}}}{1 - \eta} \quad (1)$$

where  $R_{\text{raw}}$  and  $R_{\text{con}}$  are the  $^{85}\text{Kr}/^{83}\text{Kr}$  ratio measured directly in the experiment and the  $^{85}\text{Kr}/^{83}\text{Kr}$  ratio of the Kr contaminant respectively.  $\eta$  is the volume fraction of the contamination.

Since all samples have similar sizes and are measured under the same conditions, the contamination fraction  $\eta$  for each sample should be similar as well. Therefore a single parameter  $\eta$  is used for all samples in the contamination correction model. The  $^{85}\text{Kr}/^{83}\text{Kr}$  ratio of the contaminant ( $R_{\text{con}}$ ) depends on the previous samples measured by the ATTA system and can be expressed as a weighted average of their  $^{85}\text{Kr}/^{83}\text{Kr}$  ratios. The contribution of each previously measured sample is proportional to its outgassing rate in the current measurement. The physical processes of outgassing include desorption, diffusion and permeation. The behavior of the outgassing over time under constant pumping can be generally described with a power law model  $Q_0 \times t^{-\alpha}$ , where  $Q_0$  is the initial outgassing rate right after the measurement. The power index  $\alpha$  depends on the outgassing process. The value of  $\alpha$  is about 1 if the outgassing is mainly due to desorption and is 0.5 if diffusion is dominant.<sup>36</sup> Based on this model, the  $^{85}\text{Kr}/^{83}\text{Kr}$  ratio of the contaminant in the  $n^{\text{th}}$  measurement ( $R_{\text{con}}(n)$ ) can be expressed as the following,

$$R_{\text{con}}(n) = \frac{\sum_{i=1}^{n-1} R_{\text{raw}}(i) Q_0(i) [(n-i)T(i)]^{-\alpha}}{\sum_{i=1}^{n-1} Q_0(i) [(n-i)T(i)]^{-\alpha}} \\ = \frac{\sum_{i=1}^{n-1} R_{\text{raw}}(i) V(i) [(n-i)]^{-\alpha}}{\sum_{i=1}^{n-1} V(i) [(n-i)]^{-\alpha}} \quad (2)$$

Here  $R_{\text{raw}}(i)$  is the  $^{85}\text{Kr}/^{83}\text{Kr}$  ratio measured directly in the  $i^{\text{th}}$  measurement.  $Q_0(i)$  is the initial outgassing rate due to the  $i^{\text{th}}$  measurement and is proportional to the sample size  $V(i)$ .  $T(i)$  is the measurement time of the  $i^{\text{th}}$  measurement and is the same in our experiment.

Corrections for all measurements are calculated based on eqn (1) and (2). To determine the parameter  $\alpha$  and  $\eta$  in our correction model, we calculate the corrected ratio  $R_{\text{sample}}$  for the three Kr standard sample measurements between 12:00 to 21:00 on Aug. 17, 2020 (Fig. 4), and minimize the sum of squares to their expected values. These data are used because the  $^{85}\text{Kr}/^{83}\text{Kr}$  ratio of these samples differ significantly from other air samples, therefore are more sensitive to cross-sample contamination and can provide better constraints to the model parameters. The procedure gives a set of values:  $\alpha = 0.36$  and  $\eta = 0.40$ . This result suggests that the cross-sample contamination in our measurement is controlled by a diffusion like process.

This set of model parameters is then used in the correction calculation for all samples. The corrected results are shown in Fig. 4 (closed diamonds). As one can see, the effects of cross-sample contamination have been largely removed and the corrected  $^{85}\text{Kr}$  activities of the two standard Kr samples measured from 5:00 to 12:00 on Aug. 18, 2020 (not used in determining  $\alpha$  and  $\eta$ ) agree with the expected value within measurement uncertainties. For the Hefei air samples, most of their  $^{85}\text{Kr}$  activities went up slightly after the correction. The measurement uncertainties also had increased moderately (from 3% to 5%). The results agree with the atmospheric  $^{85}\text{Kr}$  activity (shaded band) in Hefei based on the measurement of the weekly average air collected over a period (from Aug. 14, 2020 to Aug. 21, 2020) that covers the online monitoring experiment. It seems that the  $^{85}\text{Kr}$  activities in the online measurement might be higher than the weekly average value. However, as the difference is comparable to the measurement uncertainties and the two measurements cover different time spans (30 hours vs. one week), it is hard to conclude whether it is real or due to statistical fluctuations.

In conclusion, we have demonstrated continuous online monitoring of atmospheric  $^{85}\text{Kr}$  activities with 1.5 hour-time resolution. For each measurement, 3 L STP of air is needed. The whole measurement process is fully automated and only consumes liquid nitrogen. The detection limit of the system is about 5% of the current atmospheric  $^{85}\text{Kr}$  activity ( $\sim 0.075 \text{ Bq m}^{-3}$ ). The technology can be used for remote online monitoring of atmospheric  $^{85}\text{Kr}$  emitted by nuclear fuel reprocessing plants. As the  $^{85}\text{Kr}$  emission event usually happens in a short time span and has its own emission pattern, the high time resolution and online operation allows more effective monitoring and characterization of the  $^{85}\text{Kr}$  source.<sup>2</sup> The monitoring station can also be located further away from the source because the instant emission events won't be averaged out as in the traditional weekly average measurements.<sup>37</sup>

For future improvements, one possible upgrade is to introduce the all optical excitation method in the ATTA measurement. With the optical excitation method, the discharge source that causes cross sample contamination in the ATTA system can be removed. This will reduce the cross sample contamination by several orders of magnitude.<sup>38</sup> It will eliminate the need to do corrections on the measurement results, and hence smaller uncertainties. The progress in this direction will rely on the development of the narrow band 124 nm VUV lamp, which currently is limited by its lifetime of a few hundreds of hours.

## Author contributions

W. J., G. M. Y. and Z. T. L. conceived the study. Y. Q. C., X. Z. D., S. M. H., J. Q. G., W. J., Z. T. L., F. R. and G. M. Y. contributed to the design of the apparatus. Y. Q. C. built the apparatus with the helps from W. H. W., X. Z. D. and L. Z. C. G. and S. Y. L. built the ATTA apparatus. Y. Q. C. performed laboratory measurements. W. J., F. R., G. M. Y., Y. Q. C. analyzed the data. Y. Q. C., W. J., F. R., G. M. Y. and Z. T. L. wrote the paper with input from all authors.

## Conflicts of interest

There are no conflicts to declare.

## Acknowledgements

This work is funded by the National Natural Science Foundation of China (41727901, 11705196), National Key Research and Development Program of China (2016YFA0302200), Anhui Initiative in Quantum Information Technologies (AHY110000) and Anhui Provincial Natural Science Foundation (1808085MA11).

## Notes and references

- 1 B. Singh and J. Chen, *Nucl. Data Sheets*, 2014, **116**, 1–162.
- 2 J. Ahlswede, S. Hebel, J. O. Ross, R. Schoetter and M. B. Kalinowski, *J. Environ. Radioact.*, 2013, **115**, 34–42.
- 3 A. Bollhöfer, C. Schlosser, S. Schmid, M. Konrad, R. Purtschert and R. Kraiss, *J. Environ. Radioact.*, 2019, **205**, 7–16.
- 4 A. Kersting, C. Schlosser, S. Schmid, M. Konrad, A. Bollhöfer, K. Barry and A. Suckow, *Data Brief*, 2020, **33**, 106522.
- 5 Y. Igarashi, M. Aoyama, K. Nemoto, K. Hirose, T. Miyao, K. Fushimi, M. Suzuki, S. Yasui, Y. Asai, I. Aoki, K. Fujii, S. Yamamoto, H. Sartorius and W. Weiss, *J. Environ. Monit.*, 2001, **3**, 688–696.
- 6 R. Scott Kemp, *J. Environ. Radioact.*, 2008, **99**, 1341–1348.
- 7 O. Ross, PhD thesis, Hamburg University, 2010.
- 8 B. Lehmann, H. Loosli, D. Rauber, N. Thonnard and R. Willis, *Appl. Geochem.*, 1991, **6**, 419–423.
- 9 W. M. Smethie, D. Solomon, S. L. Schiff and G. G. Mathieu, *J. Hydrol.*, 1992, **130**, 279–297.
- 10 B. Ekwurzel, P. Schlosser, W. M. Smethie Jr, L. N. Plummer, E. Busenberg, R. L. Michel, R. Weppernig and M. Stute, *Water Resour. Res.*, 1994, **30**, 1693–1708.
- 11 P. G. Cook and D. K. Solomon, *Water Resour. Res.*, 1995, **31**, 263–270.
- 12 R. Althaus, S. Klump, A. Onnis, R. Kipfer, R. Purtschert, F. Stauffer and W. Kinzelbach, *J. Hydrol.*, 2009, **370**, 64–72.
- 13 M. Kagabu, M. Matsunaga, K. Ide, N. Momoshima and J. Shimada, *J. Hydrol. Reg. Stud.*, 2017, **12**, 165–180.
- 14 N. Avrahamov, Y. Yechieli, R. Purtschert, Y. Levy, J. Sültenfuß, V. Vergnaud and A. Burg, *Geochim. Cosmochim. Acta*, 2018, **242**, 213–232.
- 15 J.-Q. Gu, W. Jiang, A. L. Tong, G.-M. Yang, X.-Z. Dong, F. Ritterbusch, F. Wang and J. Wang, *J. Geophys. Res.: Oceans*, 2022, **127**, e2022JC018417.
- 16 P. Zimmermann, J. Feichter, H. Rath, P. Crutzen and W. Weiss, *Atmos. Environ.*, 1989, **23**, 25–35.
- 17 I. Levin and V. Hesshaimer, *J. Geophys. Res.: Atmos.*, 1996, **101**, 16745–16755.
- 18 E. Kjellstrom, J. Feichter and G. Hoffmann, *Tellus B*, 2000, **52**, 1–18.
- 19 A. Bollhöfer, C. Schlosser, J. Ross, H. Sartorius and S. Schmid, *J. Environ. Radioact.*, 2014, **127**, 111–118.
- 20 Š. Cimbák and P. Povinec, *Environ. Int.*, 1985, **11**, 65–69.
- 21 C. Schlosser, A. Bollhöfer, S. Schmid, R. Kraiss, J. Bieringer and M. Konrad, *Appl. Radiat. Isot.*, 2017, **126**, 16–19.
- 22 P. Collon, W. Kutschera and Z.-T. Lu, *Annu. Rev. Nucl. Part. Sci.*, 2004, **54**, 39–67.
- 23 H. Loosli and R. Purtschert, in *Rare Gases*, ed. P. K. Aggarwal, J. R. Gat and K. F. Froehlich, Springer Netherlands, Dordrecht, 2005, pp. 91–96.
- 24 C. Y. Chen, Y. M. Li, K. Bailey, T. P. O'Connor, L. Young and Z.-T. Lu, *Science*, 1999, **286**, 1139–1141.
- 25 W. Jiang, K. Bailey, Z.-T. Lu, P. Mueller, T. O'Connor, C.-F. Cheng, S.-M. Hu, R. Purtschert, N. Sturchio, Y. Sun, W. Williams and G.-M. Yang, *Geochim. Cosmochim. Acta*, 2012, **91**, 1–6.
- 26 G.-M. Yang, C. Cheng, W. Jiang, Z. Lu, R. Purtschert, Y. Sun, L. Tu and S.-M. Hu, *Sci. Rep.*, 2013, **3**, 1596.
- 27 J. C. Zappala, K. Bailey, P. Mueller, T. P. O'Connor and R. Purtschert, *Water Resour. Res.*, 2017, **53**, 2553–2558.
- 28 X.-Z. Dong, F. Ritterbusch, Y.-Q. Chu, J.-Q. Gu, S.-M. Hu, W. Jiang, Z.-T. Lu, G.-M. Yang and L. Zhao, *Anal. Chem.*, 2019, **91**, 13576–13581.
- 29 C. Gao, S.-Y. Liu, J. D. Feng, S.-M. Hu, W. Jiang, Z.-T. Lu, F. Ritterbusch, W.-H. Wang, G.-M. Yang and L. U. Zhao, *J. Environ. Radioact.*, 2021, **233**, 106604.
- 30 R. Yokochi, L. J. Heraty and N. C. Sturchio, *Anal. Chem.*, 2008, **80**, 8688–8693.
- 31 L.-Y. Tu, G.-M. Yang, C.-F. Cheng, G.-L. Liu, X.-Y. Zhang and S.-M. Hu, *Anal. Chem.*, 2014, **86**, 4002–4007.
- 32 S. Péron, S. Mukhopadhyay and M. Huh, *J. Anal. At. Spectrom.*, 2020, **35**, 2663–2671.
- 33 J. Cann, *Earth Planet. Sci. Lett.*, 1982, **60**, 114–116.
- 34 N. Aoki and Y. Makide, *Chem. Lett.*, 2005, **34**, 1396–1397.
- 35 W. Jiang, S.-M. Hu, Z.-T. Lu, F. Ritterbusch and G.-M. Yang, *Quat. Int.*, 2020, **547**, 166–171.
- 36 K. Jousten, *Handbook of Vacuum Technology* 2nd edn, Wiley, 2016.
- 37 M. B. Kalinowski, H. Sartorius, S. Uhl and W. Weiss, *J. Environ. Radioact.*, 2004, **73**, 203–222.
- 38 J. S. Wang, F. Ritterbusch, X.-Z. Dong, C. Gao, H. Li, W. Jiang, S.-Y. Liu, Z.-T. Lu, W.-H. Wang, G.-M. Yang, Y.-S. Zhang and Z.-Y. Zhang, *Phys. Rev. Lett.*, 2021, **127**, 023201.